Available online at www.sciencedirect.com
ScienceDirect
International Journal of Heat and Mass Transfer 51 (2008) 378–382
International Journal of HEAT and MASS TRANSFER
www.elsevier.com/locate/ijhmt

Technical Note

Numerical analysis of two contaminants removal from a three-dimensional cavity

Di Liu, Fu-Yun Zhao, Guang-Fa Tang *

College of Civil Engineering, Hunan University, Changsha, Hunan 410082, China

Received 25 April 2007; received in revised form 18 September 2007
Available online 26 November 2007

Abstract

This paper reports the results of a numerical study on removal of two contaminants from a three-dimensional enclosure with one inlet, one exhausting port and one returning port. In the formation of the problem, use is made of Reynolds stress model (RSM). The governing equations are solved by means of the SIMPLE algorithm. Lots of cases have been studied for the sensitivity analysis, including more practical cases from the total fresh air supplying to the total recirculation situations. The influence of inlet velocity, fresh air ratio, recirculating air filtered removal efficiency and contaminant property is investigated. The indoor contaminant is studied parametrically as a function of governing dimensionless numbers (Reynolds number and Schmidt number). The results show the above parameters have complex influence to indoor contaminant removal.

Keywords: Numerical simulation; Enclosure airflow; Air exchange rate; Contaminant removal; Heat recovery

1. Introduction

The generation of contaminants is one of the major contributing factors linked to the poor indoor air quality problem [1]. Furthermore, indoor contaminant levels are always greater than those of outdoor. Therefore, their levels can be reduced by dilution either through increased fresh air or through increased filtration [2,3].

However, increasing fresh air blindly would result in the extravagance of energy consumption. Thus, meeting the contradiction between energy conservation and comfortable indoor environment is an urgent task for researchers [1,4]. The waste heat of indoor exhaust air can be recovered by installation of heat transfer equipment [5,6]. This work aims to identify optimal air conditioning systems of providing a comfortable indoor air environment with the lowest cost of energy. Three-dimensional simulation is performed to evaluate the removal of two contaminants from an enclosure with one inlet, one exhausting port and one returning port.

2. Problem formulation

The novel window-type room air conditioner (NWRAC) considered here is composed of a window-type room air conditioner and a fan-assisted stack exhaust with pre cooling/heating of supply air by heat exchange between the indoor exhausting air and outdoor fresh air [5,6]. The supplying, recirculation and exhaust grilles are the same dimensions of 0.4 m × 0.5 m. In addition, recirculated air is mixed with the precooling/preheating fresh air to bring the total flow rate up [6]. As shown in Fig. 1, a discrete source of contaminant is located on the center of the floor, which is assumed emitting two pollutants simultaneously for constant concentration. CO_2 and HCHO have been selected as representative indoor pollutants. The outdoor pollutants are negligible.

Room airflow is governed by the three-dimensional, steady, incompressible Navier–Stokes and mass species

* Corresponding author. Tel.: +86 731 8822760; fax: +86 731 8822667.
E-mail addresses: liudi66@163.com (D. Liu), zfycfdnet@163.com (F. -Y. Zhao), gftangcfd@163.com (G.-F. Tang).

0017-9310/$ - see front matter © 2007 Elsevier Ltd. All rights reserved.
doi:10.1016/j.ijheatmasstransfer.2007.10.002

Nomenclature

C	contaminant concentration
Re	Reynolds number
Q	air flow rate
r	fresh air ratio
r_e	filtered removal efficiency
Sc	Schmidt number
x, y, z	cartesian coordinates

Greek symbols

v	kinematics viscosity
v_t	turbulent viscosity

Subscripts

exh	exhaust
fre	fresh air
mix	mixture
recir	recirculation
sou	contaminant source
sup	supply

Superscripts

CO_2	carbon dioxide
HCHO	formaldehyde

equations [7]. RSM (Reynolds Stress Model) turbulence modeling closure has been employed [8]. Cavity height H, supplying velocity u_{sup}, and concentration difference Δc ($c_{source} - c_{fre}$) are adopted for length, velocity and concentration scales, respectively [9],

$$(X_i) = (x_i)/H, (U_i) = (u_i)/u_{sup} \tag{1a}$$

$$C^{CO_2} = (c^{CO_2} - c^{CO_2}_{fre})/\Delta c^{CO_2},$$

$$C^{HCHO} = (c^{HCHO} - c^{HCHO}_{fre})/\Delta c^{HCHO}, \quad P = p/\rho u^2_{sup} \tag{1b}$$

$$k = \frac{k^*}{u^2_{sup}}, \quad \varepsilon = \frac{\varepsilon^* H}{u^3_{sup}} \tag{1c}$$

The corresponding control parameters are as follows:

$$Re = u_{sup}H/v, \quad Sc^{CO_2} = v/D^{CO_2},$$

$$Sc^{HCHO} = v/D^{HCHO} \tag{2}$$

Schmidt numbers with 0.2 (CO_2) and 2.0 (formaldehyde) have been considered [10]. For the inlet section, the Reynolds number is in a range of 10^2–10^5.

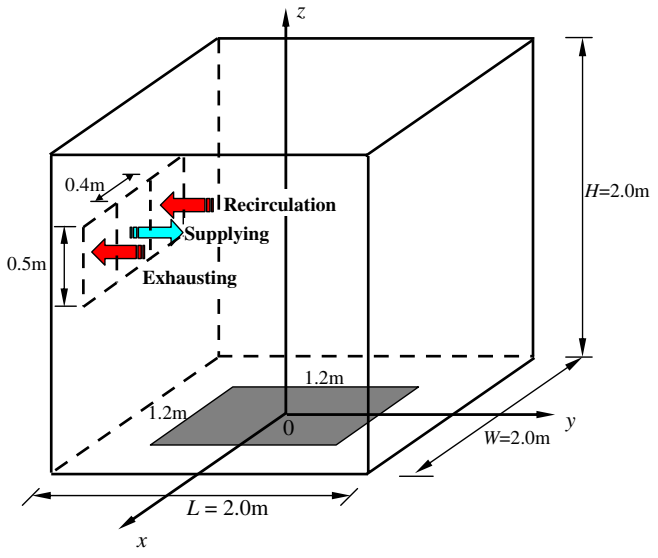

Fig. 1. Schematic diagram of the simulated room with novel window-type air conditioner.

The non-slip impermeable condition is imposed on all the solid walls. $V_{sup} = W_{sup} = 0$, $U_{sup} = 1$ representing the mean stream wise longitudinal dimensionless velocity. $k_{sup} = 3/2(u_{sup}I_{ox})^2$, where $I_{ox} = 10\%$ represents the turbulence intensity of the X-component of velocity at the inlet as obtained from experiments. $\varepsilon_{sup} = (C^{0.75}_{\mu}k^{1.5}_{sup}/0.07D_H)$, where D_H represents the hydraulic diameter of the inlet section. The turbulence is assumed to be isotropic, $\overline{u'_i u'_j} = \frac{2}{3}k_0\delta_{ij}$. Zero flux outlet boundary conditions were chosen for k and ε. Close to the wall, where viscous effects become dominant, these turbulence models are used in conjunction with wall functions [8].

Concerning the constituent conservation for the NWRAC, the velocity boundary conditions of outlet are given below,

$$U_{recir} = (1 - r)U_{sup}, \quad U_{exh} = rU_{sup} \tag{3}$$

where the fresh air ratio is defined as $r = Q_{fre}/Q_{sup}$ ($0 < r < 1$). In terms of no filtration of carbon dioxide, $r_e = 0$, the concentration boundary conditions are,

$$C^{CO_2}_{sup} = (1 - r)C^{CO_2}_{recir} = (1 - r)\frac{\int_{A_{recir}} c^{CO_2}_{recir}\,dA}{A_{recir}} \tag{4}$$

$$\left.\frac{\partial C}{\partial n}\right|^{CO_2}_{recir} = \left.\frac{\partial C}{\partial n}\right|^{CO_2}_{exh} = 0 \tag{5}$$

In terms of filtration of formaldehyde,

$$C^{HCHO}_{sup} = (1 - r)(1 - r_e)C^{HCHO}_{recir} = (1 - r)(1 - r_e)\frac{\int_{A_{recir}} c^{HCHO}_{recir}\,dA}{A_{recir}} \tag{6}$$

$$\left.\frac{\partial C}{\partial n}\right|^{HCHO}_{recir} = \left.\frac{\partial C}{\partial n}\right|^{HCHO}_{exh} = 0 \tag{7}$$

The numerical method used in this work is a three-dimensional turbulent version of the control-volume based finite difference procedure described in [7,9,11–13]. All calculations carried out in this work are based on $42 \times 42 \times 42$ control volumes. The current numerical method has been successfully used in a series of recent papers [9,11–18]. For

turbulent lid-driven flow in a three-dimensional cavity, the numerical results were in excellent agreement with the experiments given by Koseff and Street [19].

3. Results and discussion

3.1. Effect of Reynolds number

Side-viewing of $Y = 0$, there are two main flow patterns formed in the enclosure, the lower one is a clockwise recirculation zone near the floor, and the upper counterclockwise circulates near the roof (Fig. 2). The two zones are directly separated by the supplying jet. The higher *Re* results in the longer persisting extended distance, with mixing pollutants. Passing over the whole room, pollutants emitted from the floor source are entrained into the clockwise cell and taken away from the cavity following the fluid flow. The concentration of CO_2 is reduced with increasing *Re*, and tends to constant for $Re > 10^5$. Correspondingly, dilution is an increasing function with *Re*. For HCHO with $r_e = 0.8$, the inlet coming wind always brings the low concentration level even $Re = 10^2$.

Observing from the Fig. 2, when *Re* is low ($<10^4$), the concentration field that rides on the forced convection depends to a significant degree on Sc. For CO_2, the concentration boundary layers are non-distinct and mass transfer through the cavity is mainly by diffusion in the vertical direction. The opposite effect is encountered for HCHO, where the concentration boundary layers become sharper than that of CO_2. In addition, for formaldehyde, the mass diffusivity is low enough such that the vertical intrusion layers lining the sidewalls are considerably sharper than that counterpart of CO_2, the net result is that the core of the HCHO concentration field is in a state of uniform concentration. When *Re* is sufficiently high ($>10^5$), and the flow circulation is driven mostly by the supply velocity and the results are independent of Schmidt effect.

3.2. Effect of fresh air ratio

Without fresh air, the recirculation port results in the strong indraft being confined within narrow zone. Upon increasing *r* from zero, the increasing velocity of the exhaust port results in the enlargement of the confined zone (Fig. 3). Simultaneously, a weak counter-clockwise cell develops in the front left corner, while the incoming jet stretches (becomes straighter and thinner) near the back wall. The incoming clean air bypasses the rest of the enclosure and proceeds directly toward the outlet. The role of the fresh air ratio is to reduce and dilute the indoor pollutants. With no fresh air and filtration, the accumulation occurs. As *r* increases, the CO_2 concentration of incoming flow decreases at the supply location. For HCHO (with filtration $r_e > 0$), even without fresh air, the indoor contaminant concentration is acceptable. This means that fresh air and filtration are both the effective ways to improve the indoor environment.

When CO_2 ($r_e = 0$) is carried away by the jet (Fig. 3), an almost linear variation of the average pollutant level prevails, and the removal efficiency represented as the reciprocal of average pollutant level increases abruptly. Thereafter, a small decrease of contaminant concentration is observed. The CO_2 concentration is consistently decreasing in order of increasing fresh air ratio, but the decreasing rate becomes less. For formaldehyde without filtration, the

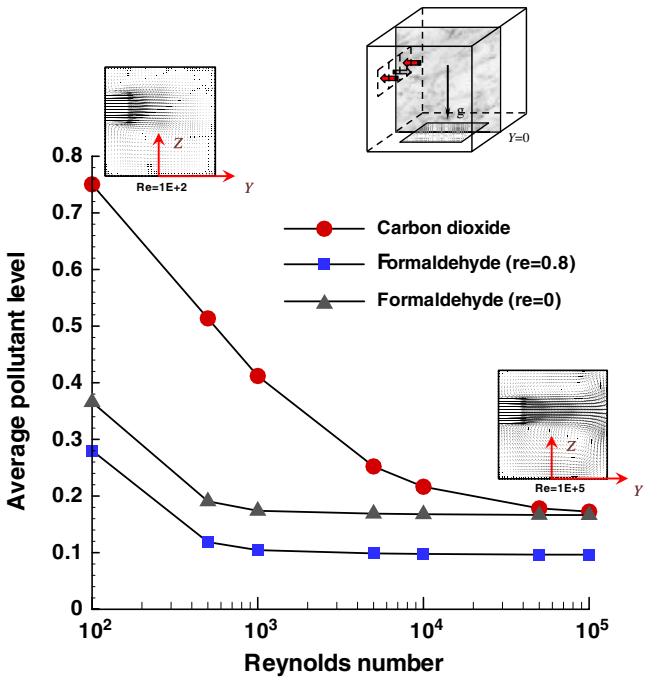

Fig. 2. Variation of average pollutant level with Reynolds number as parameter for fresh air ratio $r = 0.5$.

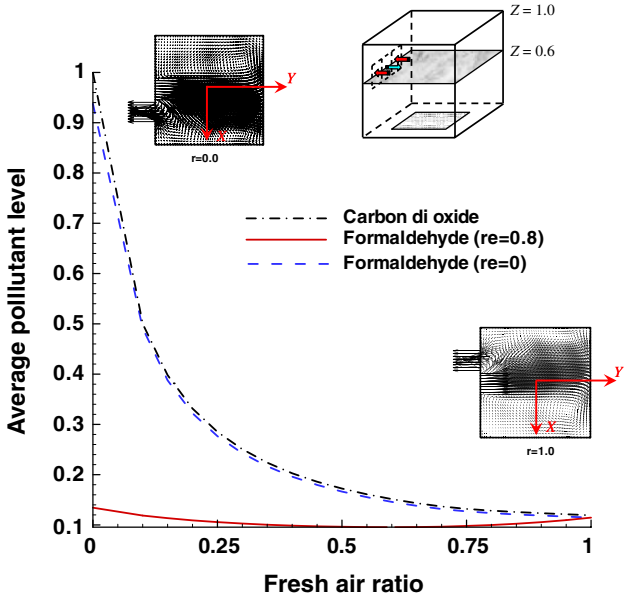

Fig. 3. Variation of average pollutant level with fresh air ratio *r* as parameter for $Re = 10^5$.

average pollutant level and its trend are almost the same with that of CO_2. This is due to that Reynolds number is sufficiently high (10^5), and the flow circulation is driven mostly by the inlet supply velocity and the results are independent of the Schmidt effect. While, the concentration of formaldehyde under filtration condition ($r_e = 0.8$) is first slightly decreasing until $r = 0.5$, which is the minimal pollutant level, and then increasing. The highest average formaldehyde level is about 0.13, much lower than that of contaminant without filtration [4]. The average pollutant level with or without filtration approaches the same level with $r = 1.0$. It attributes to the continuous release of the contaminant. The result agrees well with the constituent conservation analysis (Eq. (8)).

$$\lim_{n\to\infty} C_n = \lim_{n\to\infty} C_{\mathrm{mix}(n)} = \frac{C_1}{1-(1-r)(1-r_e)} \tag{8}$$

where C_1 represents the concentration of recirculating port for the first recirculation.

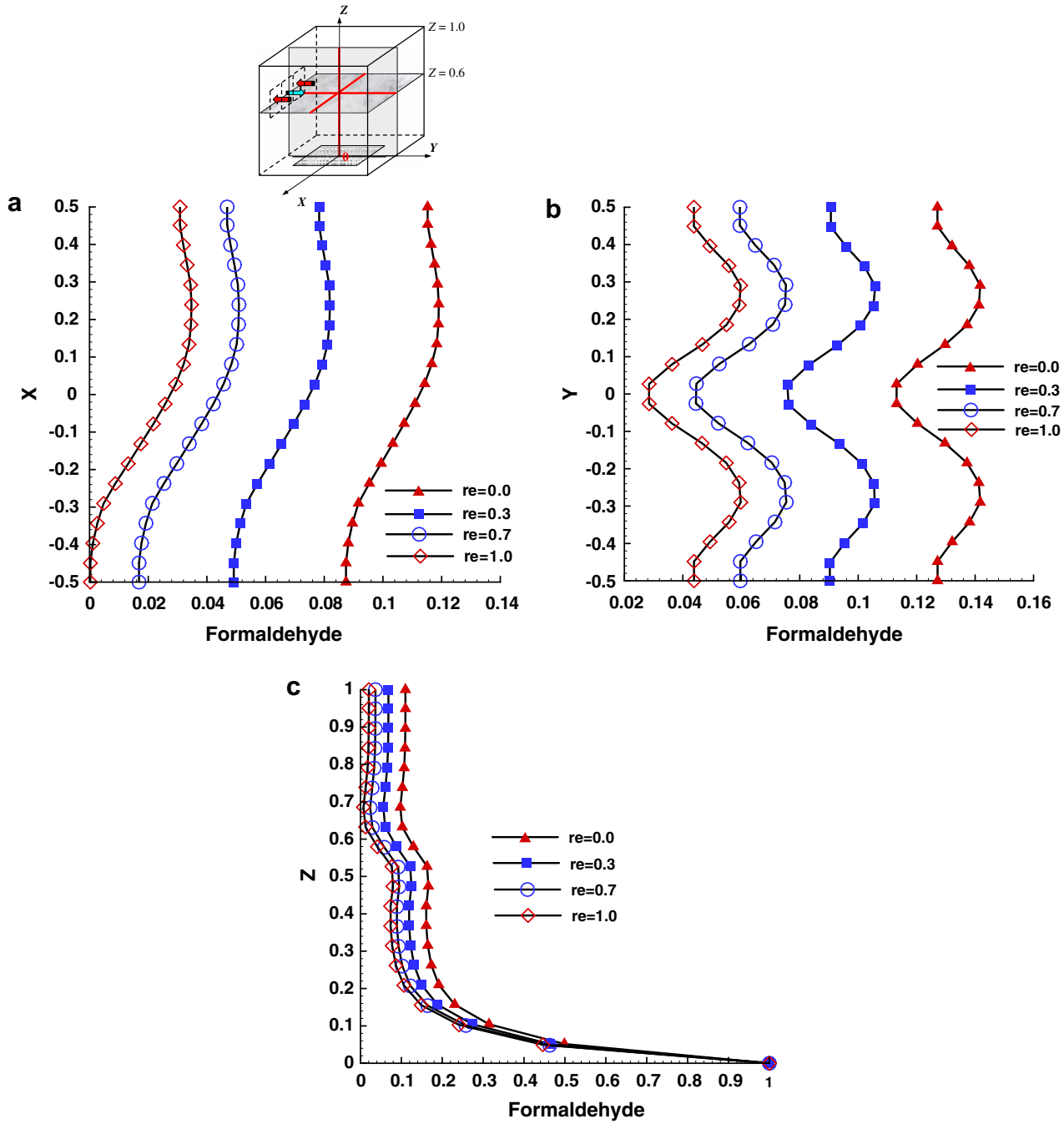

Fig. 4. The iso-concentration profiles. (a) In the Z-plane ($Z = 0.6$) along the horizontal line (X direction) $Y = 0.0$, (b) in the Z-plane ($Z = 0.6$) along the horizontal line (Y direction) $X = 0.0$ and (c) in the mid-Y-plane ($Y = 0.0$) along the vertical line (Z direction) $X = 0.0$. Evolution of center concentration profiles of formaldehyde for various filtered removal efficiency r_e.

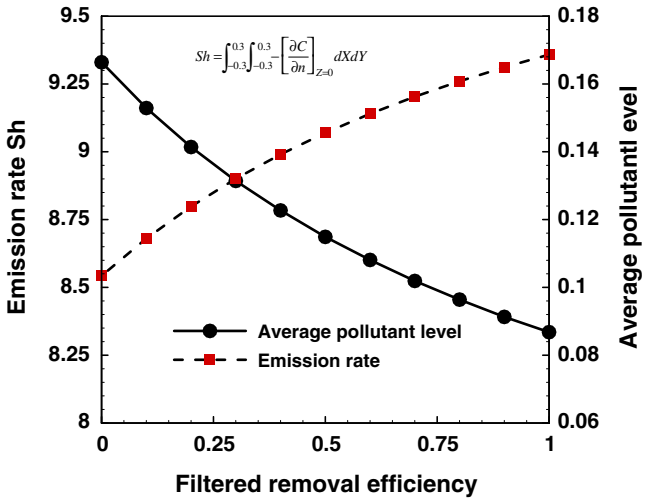

Fig. 5. The average pollutant level and emission rate of formaldehyde with different filtered removal efficiencies r_e for $Re = 10^5$ and fresh air ratio $r = 0.5$.

3.3. Effect of filtered removal efficiency

For CO_2 cannot be filtered, this section focuses on formaldehyde. Fig. 4a–c indicates an area of high concentration in recycling region due to the interaction of the primary and secondary flow cells. The results show that formaldehyde emitted from the floor tends to follow the course of the airfield moving circularly. It can be seen that the minimum is at the inlet and quickly increases along the length. We can see a higher and uniform concentration distribution after $X = 0$. The formaldehyde concentration is a step increasing function for r_e as parameter. The lower r_e, the more the pollutant will be accumulated within the enclosure. The double peak structures observed in Y-direction concentration profiles illuminate the accumulation on the recirculating and exhausting sides. The Z-direction concentration profiles indicate the sharply decreasing just above the floor, and then slowly decreasing along the height.

With an increase in the filtered removal efficiency, the average concentration decreases (Fig. 5). This means that the higher filtered removal efficiency, the less pollutant can move into the room. The emission rate of formaldehyde is also affected by the filtered removal efficiency. Reversing from the volumetric average concentration, the emission rate is an increasing function with the filtered removal efficiency.

4. Conclusions

The effects of Reynolds number, Schmidt number, filtered removal efficiency and fresh air ratio are studied numerically. The results show that increasing Reynolds number reduces the average pollutant levels effectively. The concentrations of pollutants with different molecular diffusivity approach to the same value for fresh air ratio tend to be unity. The HCHO level is a decreasing function with filtered removal efficiency.

Acknowledgement

This work was supported by the National Natural Science Foundation of China (No. 50578059). The constructive comments of the reviewers are also highly appreciated.

References

[1] M. Soria, A. Oliva, M. Costa, et al., Effect of contaminant properties and temperature gradients on the efficiency of transient gaseous contaminant removal from an enclosure: a numerical study, Int. J. Heat Mass Transfer 30 (1998) 2609–3589.
[2] H.A. Aglan, Prediction model for CO_2 generation and decay in building envelopes, J. Appl. Phys. 93 (2003) 1287–1290.
[3] M. Abadie, K. Limam, F. Allard, Indoor particle pollution: effect of wall textures on particle deposition, Build. Environ. 36 (2001) 821–827.
[4] A. Elkilani, W.S. Bouhamra, Estimation of optimum requirements for indoor air quality and energy consumption in some residences in Kuwait, Environ. Int. 27 (2001) 443–447.
[5] D. Liu, G.F. Tang, F.Y. Zhao, Modeling and experimental investigation of looped separate heat pipe as waste heat recovery facility, Appl. Therm. Eng. 26 (2006) 2433–2441.
[6] D. Liu, F.Y. Zhao, G.F. Tang, Frosting of heat pump with heat recovery facility, Renew. Energy 32 (2007) 1228–1242.
[7] S.V. Patankar, Numerical Heat Transfer and Fluid Flow, Hemisphere, Washington DC, 1980.
[8] B.E. Launder, G.J. Reece, W. Rodi, Progress in the development of a Reynolds stress turbulence closure, J. Fluid Mech. 68 (1975) 537–566.
[9] F.Y. Zhao, G.F. Tang, D. Liu, Conjugate natural convection in enclosures with external and internal heat sources, Int. J. Eng. Sci. 44 (2006) 148–165.
[10] C. Beghein, F. Haghighat, F. Allard, Numerical study of double-diffusive natural convection in a square cavity, Int. J. Heat Mass Transfer 35 (1992) 833–846.
[11] F.Y. Zhao, D. Liu, G.F. Tang, Application issues of the streamline, heatline and massline for conjugate heat and mass transfer, Int. J. Heat Mass Transfer 50 (2007) 320–334.
[12] F.Y. Zhao, D. Liu, G.F. Tang, Conjugate heat transfer in square enclosures, Heat Mass Transfer 43 (2007) 907–922.
[13] F.Y. Zhao, D. Liu, G.F. Tang, Free convection from one thermal and solute source in a confined porous medium, Transport Porous Media (2007), doi:10.1007/s11242-007-9106-7.
[14] D. Liu, F.Y. Zhao, G.F. Tang, Conjugate heat transfer in an enclosure with a centered conducting body imposed sinusoidal temperature profiles on one side, Numer. Heat Transfer Part A (2007), doi:10.1080/10407780701454030.
[15] F.Y. Zhao, D. Liu, G.F. Tang, Multiple steady flows in confined gaseous double diffusion with discrete thermosolutal sources, Phys. Fluids (2007), doi:10.1063/1.2770518.
[16] F.Y. Zhao, D. Liu, G.F. Tang, Resonant response of fluid flow subjected to discrete heating elements, Energy Convers. Manage. 48 (2007) 2461–2472.
[17] F.Y. Zhao, D. Liu, G.F. Tang, Natural convection in a porous enclosure with a partial heating and salting element, Int. J. Therm. Sci. (2007), doi:10.1016/j.ijthermalsci.2007.04.006.
[18] D. Liu, F.Y. Zhao, G.F. Tang, Thermosolutal convection in a saturated porous enclosure with concentrated energy and solute sources, Energy Convers. Manage. (2007), doi:10.1016/j.enconman.2007.06.003.
[19] J.R. Koseff, R.L. Street, The lid-driven cavity flow: a synthesis of qualitative and quantitative observations, ASME J. Fluid Eng. 106 (1984) 390–398.